Electronic version of an article published as International Journal of Neural System. 2018 Jun;28(5):1750017. doi: 10.1142/S0129065717500174. Epub 2017 Jan 10

A MULTIPLE-PLASTICITY SPIKING NEURAL NETWORK EMBEDDED IN A CLOSED-LOOP CONTROL SYSTEM TO MODEL CEREBELLAR PATHOLOGIES

ALICE GEMINIANI[†], CLAUDIA CASELLATO*, ALBERTO ANTONIETTI[‡]
NeuroEngineering and Medical Robotics Laboratory, Department of Electronics, Information and Bioengineering, Politecnico di Milano, P.zza Leonardo Da Vinci 32, 20133, Milano, Italy
[†]*alice.geminiani@polimi.it*
**claudia.casellato@polimi.it*
[‡]*alberto.antonietti@polimi.it*

EGIDIO D'ANGELO
Department of Brain and Behavioral Sciences, University of Pavia, Via Forlanini 6, I-27100, Pavia, Italy
Brain Connectivity Center, Istituto Neurologico IRCCS Fondazione C. Mondino, Via Mondino 2, I-27100, Pavia, Italy
egidiougo.dangelo@unipv.it

ALESSANDRA PEDROCCHI
Neuroengineering and Medical Robotics Laboratory, Department of Electronics, Information and Bioengineering, Politecnico di Milano, P.zza Leonardo Da Vinci 32, 20133, Milano, Italy
alessandra.pedrocchi@polimi.it

The cerebellum plays a crucial role in sensorimotor control and cerebellar disorders compromise adaptation and learning of motor responses. However, the link between alterations at network level and cerebellar dysfunction is still unclear. In principle, this understanding would benefit of the development of an artificial system embedding the salient neuronal and plastic properties of the cerebellum and operating in closed-loop. To this aim, we have exploited a realistic spiking computational model of the cerebellum to analyse the network correlates of cerebellar impairment. The model was modified to reproduce three different damages of the cerebellar cortex: (i) a loss of the main output neurons (Purkinje Cells), (ii) a lesion to the main cerebellar afferents (Mossy Fibers), and (iii) a damage to a major mechanism of synaptic plasticity (Long Term Depression). The modified network models were challenged with an Eye-Blink Classical Conditioning test, a standard learning paradigm used to evaluate cerebellar impairment, in which the outcome was compared to reference results obtained in human or animal experiments. In all cases, the model reproduced the partial and delayed conditioning typical of the pathologies, indicating that an intact cerebellar cortex functionality is required to accelerate learning by transferring acquired information to the cerebellar nuclei. Interestingly, depending on the type of lesion, the redistribution of synaptic plasticity and response timing varied greatly generating specific adaptation patterns. Thus, not only the present work extends the generalization capabilities of the cerebellar spiking model to pathological cases, but also predicts how changes at the neuronal level are distributed across the network, making it usable to infer cerebellar circuit alterations occurring in cerebellar pathologies.

Keywords: cerebellum; Spiking Neural Networks; pathological models; synaptic plasticity; eye blink conditioning.

1. INTRODUCTION

The brain architecture encompasses large-scale networks organized in closed-loop, in which the strength of signal communication is continuously adjusted through synaptic plasticity. This anatomo-functional organization eventually allows to regulate the information processing required to drive adaptive behavior, as indicated by a wealth of physiological and pathological data and by theoretical motor control models.[1,2] A critical element in

the control loop is the cerebellum[3–5], which implements three fundamental operations: prediction, timing and learning of motor commands.[6–10] These properties emerge in associative sensorimotor paradigms, such as the Eye-Blink Classical Conditioning (EBCC). This Pavlovian associative task is learned along with repeated presentations of paired stimuli, a Conditioned Stimulus (CS, like a tone) followed after a fixed Inter Stimulus Interval (ISI) by an Unconditioned Stimulus (US, like an air-puff or an electrical stimulation), eliciting the eye-blink reflex. The cerebellum learns to produce a Conditioned Response (CR, an eye-blink) precisely timed to anticipate (or "predict") the US onset.[11]

In the present work, we have exploited a detailed computational model of the cerebellum, embedded in a sensorimotor circuit and operating in closed-loop, to reproduce three prototypical pathological conditions of the cerebellar cortex and simulate the corresponding behavioral alterations. The model, a realistic Spiking cerebellar Neural Network (SNN)[12–16], included detailed neuron models with proportionate population sizes and appropriate connection ratios. The model was connected to an external sensori-motor circuit capable of processing the EBCC. The model plasticity sites were distributed in both cortical and nuclear layers.[17] Long-Term Depression (LTD) or Long-Term Potentiation (LTP) mechanisms were modeled as specific modifications of synaptic conductances. The same modeling framework was developed by our research group to simulate EBCC under physiological conditions and to provide insight into different cerebellar plasticity mechanisms.[17,18] This framework establishes a solid basis for the analysis of pathological conditions in this work, as shown by preliminary proof-of-concept analyses.[19,20]

We hypothesized that, by appropriately manipulating model parameters to reproduce cerebellar deficits, we should be able to observe the corresponding behavioral effects and to predict the underlying neural circuit adaptation. If this would be proved, *in silico* simulations based on realistic computational modeling could become fundamental to formulate hypotheses on disease mechanisms and to evaluate the efficacy of treatments.[21] This could also help to overcome the actual incomplete knowledge about cerebellar diseases[22] and the limits of *in vitro* and *in vivo* analyses, bridging the gap between micro scales (cells), mesoscale (local circuits), macroscale (large-scale connection systems) and behavior.

In order to face the issue, in this study, three different prototypes of cerebellar impairment have been analyzed, each one involving a different neural population or mechanism. The first pathological model was a reduced number of Purkinje cells, which are the final integrators of all cerebellar cortex computations and also a major site of plasticity.[23] The second pathological model was characterized by a compromised input signal coming from the Mossy Fibers.[24] The last case reproduced an impairment of long-term depression, the main mechanism of supervised cerebellar cortical plasticity.[25] After tuning model parameters to simulate the standard physiological conditions, appropriate alterations were introduced in order to reproduce the pathological changes observed in humans or animals and, in these pathological cases, the EBCC was simulated and analyzed.

2. METHODS

2.1. *Computational cerebellar model and optimization*

The cerebellar model used for the simulations was based on a well-established cerebellar architecture[18,26,27], which was built on physiological features of a cerebellar microcomplex. We used the Event-Driven simulator based on Look-Up-Tables, EDLUT[28–30], an open source SNN simulator that operates by compiling the dynamic responses of pre-defined cell models into lookup tables, thus allowing real-time performance. The simulations were performed on a desktop PC (Intel® Xeon® CPU E5-1620 v2 @3.70 GHz with 32 GB of RAM and Windows 7 64 bit as Operating System).

The SNN (Fig. 1A) was composed of 300 Mossy Fibers (MFs), 6000 Granule cells (GRs), 72 Inferior Olive cells (IOs), 72 Purkinje Cells (PCs) and 36 Deep Cerebellar Nuclei (DCNs). Reproducing the EBCC loop, the MFs received the CS, as a random spike pattern with physiological frequency, and were connected with the granular layer; each GR received 2 somatotopic and 2 random excitatory synapses from the MFs. The GR activity was a sparse representation of the input signal, so each simulation time sample corresponded to a different state of the granular layer.[31] The IOs received the US as a low-frequency random spike pattern[32], not depending on the dynamics of the network but associated to the US event. The IOs were connected one by one to PCs through the Climbing Fibers (CFs). Each PC received synapses from each GR with a probability of 80%, through Parallel Fibers (PFs), resulting in 345444 connections. Each DCN

received excitatory inputs from all the MFs and 2 inhibitory connections from 2 PCs. Single neurons were modeled as Leaky Integrate and Fire[33], while the synapses were represented as input-driven conductances, with the same parameters used in previous studies.[30,34–36] Within our model, the DCN-IO inhibitory loop[37] did not correspond to a physical connection, but it was implemented as a mechanism that decreased the IO firing rate of the spike pattern representing US, if a CR was detected before the US onset. This way, such DCN-IO inhibitory loop translated the motor command into a sensory modulation, meaning that a single cerebellar area simultaneously tackled both motor execution and sensory prediction.[38,39] CR detection was based on the evaluation of the output signal *DCNoutput*, related to the DCN population firing rate. The algorithm was updated compared to previous versions of the model[18,20] in order to consider the same parameters reported in experimental studies. We evaluated both the timing and the shape of the output signal, in terms of its amplitude and slope; specifically, for each trial, a CR was identified at time t_{CR} if all the following conditions were verified (Fig. 1B):

- $lat_{max} \leq t_{CR} <$ ISI. (1)

Where $lat_{max} = \begin{cases} 200 \text{ ms}, & \text{for long ISI (e.g. 400 ms)} \\ 150 \text{ ms}, & \text{for short ISI (e.g. 250 ms)} \end{cases}$

This condition allowed excluding random responses at the beginning of each trial, which could not be related to the associative paradigm.[40–42]

- At time t_{CR} the output signal crossed the *threshold* value, linearly depending on the *baseline*:

$$threshold = 2.5 \cdot baseline + 45. \quad (2)$$

Where the *baseline* was the mean output signal in the initial interval of each trial, before lat_{max}. This way, we were able to consider only the CR resulting from an output activity significantly different from the baseline activity.[43]

- The *ratio* parameter, which accounts for the output signal's slope, overcame a constant threshold:

$$ratio = \frac{DCNoutput\,(t_{CR})}{\text{mean}(DCNoutput\,(t \leq t_{CR}))} \geq 3. \quad (3)$$

Therefore, a CR was detected only in case of a rapid increase of DCN activity, before US onset.[44]

Learning occurred thanks to synaptic plasticity, which was introduced in the three plasticity sites at both cortical and nuclear level. Cortical plasticity driving fast learning was modeled as LTP and LTD at PF-PC connections triggered by the IO teaching signal, which caused the decrease of synaptic strength 100 ms before the US-related IO activity. On the other hand, nuclear plasticity was modeled as LTP and LTD triggered by the PC activity for MF-DCN synapses, and as Spike-Timing Dependent homosynaptic Plasticity (STDP) for PC-DCN connections. These nuclear mechanisms were responsible for driving a slow consolidation of learned motor responses.

For each one of the plasticity sites, synaptic strength variation was regulated by specific learning rules with

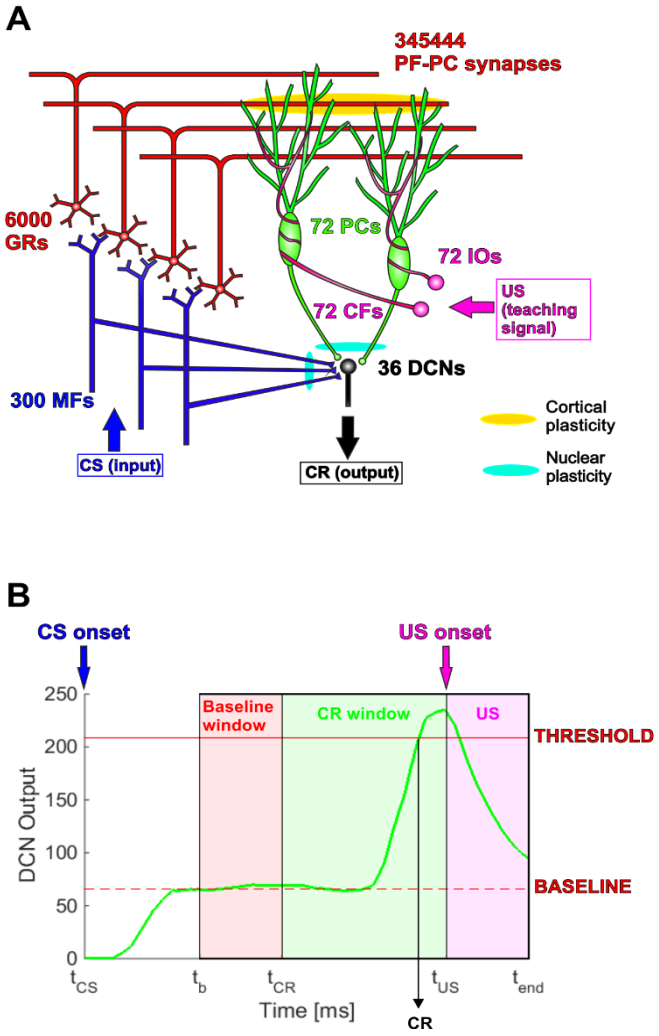

Fig. 1. (A) Cerebellar model. The SNN includes 6480 neurons, with realistic population size and connection ratios. The input signals are conveyed through MFs and IOs, whereas the output motor command is provided by the DCNs. (B) Representation of the output during one single trial. The baseline and the corresponding threshold are represented as horizontal lines. CS and US onset and the CR are highlighted. The shadowed areas indicate the different time windows considered in the CR detection algorithm.

parameters modulating the amount of LTP and LTD at cortical and nuclear sites.[18] Tuning of learning rule parameters and initial weights of the plastic connections was obtained through a Genetic Algorithm[45,46], which was based on the evaluation of EBCC simulations in order to achieve physiological behavior.[47,48] Specifically, the protocol included two learning sessions so as to evaluate the proper physiological action of the different plasticity sites on multiple time scales.[18] Referring to one of the pathological protocols[23], each session consisted of 100 acquisition and 30 extinction trials[49], with ISI = 440 ms.

After running the simulations for each one of the 12 individuals in a generation, they were assigned a fitness value based on the %CR in a moving window of 10 trials. Specifically, the fitness evaluated the behavior during both the acquisition and the extinction phases:

$$fitness = \frac{\sum_{i=1}^{2} p_{ia} \cdot p_{ie}}{penalty}. \quad (4)$$

Where, i indicates the session, a = acquisition, e = extinction, p and *penalty* are functions defined as follows:

$$p_{ij} = \begin{cases} k_j \cdot \boldsymbol{t_{ij}} + \delta, & \text{if } 0 < \boldsymbol{t_{ij}} < th_{min,ij} \\ p_{max,j}, & \text{if } th_{min,ij} \le \boldsymbol{t_{ij}} \le th_{max,ij} \\ th_{max,ij} - \left(\frac{\boldsymbol{t_{ij}} - th_{max,ij}}{\partial_j}\right)^3 \cdot \left(th_{max,ij} - th_{min,ij}\right), & \\ \quad \text{if } \boldsymbol{t_{ij}} > th_{max,ij} & \end{cases} \quad (5)$$

Where $\boldsymbol{t_{ij}}$ is the first trial when %CR reached a certain threshold during the phase j (acquisition or extinction) of session i (1 or 2), the thresholds $th_{min,ij}$ and $th_{max,ij}$ were chosen to obtain acquisition and extinction in a physiological number of trials (Table 1), the constants k_j, δ and ∂_j were established to rescale the term p_{ij}, and the maximum value $p_{max,j}$ was 1 for acquisition and 0.5 for extinction, in order to weigh the first phase more, since a lack of acquisition is a more severe non physiological behavior.

The denominator of *fitness* was built so as to avoid saturation of %CR at 100%, which is unusual and would prevent further learning modulation:

$$penalty = \begin{cases} 1, & \text{if } tot_{100\%\,CR} < 20 \\ 1 - c \cdot tot_{100\%\,CR}, & \text{if } tot_{100\%\,CR} \ge 20 \end{cases} \quad (6)$$

Where $tot_{100\%CR}$ was the total number of trials with 100% of CRs and c was a normalization constant.

The resulting maximum value for *fitness* was 1.

Table 1. Minimum and maximum threshold trials for each phase (acquisition and extinction) of sessions 1 and 2.

	$\boldsymbol{th_{min,ij}}$	$\boldsymbol{th_{max,ij}}$
acq1	10	50
ext1	105	120
acq2	140	180
ext2	235	250

Based on the fitness values, the roulette wheel selection method was then applied and the obtained parents underwent one-point crossover and mixed mutation (to achieve elitism, exploration and exploitation of the search space). Specifically, the first four best individuals were kept in the following generation, other four ones were obtained through uniform mutation and the remaining ones through Gaussian mutation. As stop criteria, we chose a maximum total number of generations and a maximum number of generations without any significant improvement of the best individual's fitness. After one of the stop criteria was met, the final parameters were chosen considering all the individuals that achieved the maximum fitness value (=1) and then computing the mean values of their genes. In fact, as the fitness function was not specific, there were multiple parameter combinations resulting in a physiological performance, and their mean values represented the best solution in an intermediate optimal region. To prove the robustness of the obtained parameters, we tested them on EBCC simulations with a shorter ISI of 250 ms.

2.2 *Protocol and Pathology impairments*

All tests were performed on the delay EBCC task (CS and US coterminate) after specific manipulations of the optimized physiological model, and the protocol parameters (stimuli durations, ISI, number of trials) were set to reproduce the same conditions as in the reference pathological studies. Then, for all the three pathology cases, we performed also simulations on a longer acquisition protocol, in order to make hypotheses on the evolution of behavior on a slow time scale. To evaluate the outcome of the model during both physiological and pathological situations, we computed the mean and SE (Standard Error) of the total number of CRs (#CR) produced along all the acquisition trials for different lesion amounts; moreover we evaluated the CRs incidence as the mean and SE of %CR on blocks of 10 trials, for the multiple pathological simulations with the same damage

amount. Besides CRs generation, also the timing of the response is a fundamental parameter characterizing a proper learning.[44] Therefore, we considered also the onset and peak latencies of CRs: onset latency was a negative value defined as the time interval, prior to US onset, when *DCNoutput* firstly overcame the *baseline* value, after lat_{max}. Peak latency was defined as the time interval (negative value) between US onset and the CR-detection time, t_{CR}. For all cases, the non-parametric Wilcoxon-Mann-Whitney statistical test was performed to evaluate the response timing modifications between healthy and pathological outcomes. We then considered the low-level mechanisms, by analyzing the *DCNoutput* and the evolution of synaptic weights. Specifically, for the three plasticity sites we represented the histograms of the conductance values at the beginning and the end of the learning protocol. We also fitted the histograms with a normal distribution and compared the mean values of the final weights for healthy and pathological behaviors through the parameter Δ_i:

$$\Delta_i = \frac{\text{mean\_path}_i - \text{mean\_healthy}_i}{\text{range}_i} \cdot 100, \quad i = \text{PFPC, MFDCN, PCDCN} \tag{7}$$

We considered non-significant an absolute value lower than 1%.

Then, we also represented the firing patterns of PCs and DCNs, involved in the learning process. We computed the number of spikes in time bins of 10 ms during the whole duration of all the acquisition trials.

2.2.1 Loss of Purkinje cells

The first investigated case concerned a damage to a cerebellar neural population at cortical level, the PCs. Their role in motor adaptation has been proved crucial for learning, because they directly influence the DCN output through an inhibitory signal and their activity is controlled by cortical plasticity, which is the main fast learning mechanism. Therefore, PC loss produces severe damage on motor learning as demonstrated by studies on cerebellar cortical degeneration, with different extents of compromised PC volumes, which characterize some typical cerebellar pathologies.[40,50,51] In this case, the delay EBCC paradigm is a common tool to evaluate motor impairment: a damage to PCs causes the DCNs to generate an inappropriate output, outside the physiological time window of associative responses, resulting in reduced conditioning and shorter latency of CRs. In particular, in Ref. 23 they used EBCC to evaluate motor learning impairment on 25 patients suffering from cerebellar cortical degeneration, with 20% of PC volume reduction. Each subject underwent 100 CS-US acquisition trials with ISI = 440 ms, followed by 30 CS-alone extinction trials.

To simulate analogous conditions, we carried out EBCC simulations of the acquisition phase with the same protocol parameters, using a modified model that included a decreased number of PCs, ranging from 3 to 27 removed PCs, i.e. from 4% to 37% of the reference value in physiological conditions. For each amount of removed PCs, 36 tests were performed, with different templates of lost PCs (spatial patterns). We compared the model outcome with the results of the reference study and we predicted the modified underlying mechanisms through the analysis of the output activity and the synaptic weights. Moreover, we performed tests with 1000 acquisition trials to hypothesize the behavior on a longer time scale.

2.2.2 Impaired cerebellar afferents

This case concerned a study on a patient with damage to cerebellar input pathways, due to a cerebrovascular accident.[24] In particular, the woman showed evidence of alterations at Pontine areas, which are the main afferents to the cerebellum. Because of this damage, when performing EBCC the patient was not able to acquire CRs. While control subjects reached 80% of CRs (computed on blocks of 10 trials), the woman maximum value was 20%, over a training session of 100 paired presentations of CS and US, with ISI = 400 ms; therefore, learning was compromised or at least severely delayed.

To simulate the same situation in the cerebellar model, two solutions have been implemented: a reduction in the number of active MFs or a decrease in the MF firing rate during CS. The explored impairment level ranged from 5% to 50% of the reference value in physiological conditions and 36 tests were performed for each lesion amount, with different spatial patterns of MF damage. The protocol for *in silico* simulations of both physiological and pathological conditions was the same as in the reference case: CS = 500 ms, US = 100 ms co-terminating with CS, ISI = 400 ms, 10 blocks of 10 trials, with one CS-alone and 9 CS-US repetitions. Then, the outcomes of both normal and altered models were compared, in terms of response generation, timing and low-level activity.

In order to verify whether conditioning was totally compromised or only severely delayed as suggested in Ref. 24, we run simulations with the same templates of 25% MF damage and 1000 total trials. Then we restored the

damaged model and we run another simulation with the same protocol parameters and 1000 acquisition trials, to further shed light on the role of the cortical and nuclear pathways.[52]

2.2.3 Impaired LTD at PF-PC synapses

Finally, the third case involved a damage to intrinsic working mechanisms in the cerebellum, instead of neural population or signal impairment as in the first and second cases. Cortical plasticity (at PF-PC synapses) has been recognized to have an essential role in motor learning in the cerebellum.[53–55] The reference study analysed adaptation during an EBCC task in mice reporting damaged LTD at PF-PC synapses.[25] In particular, LTD impairment at this plasticity site resulted from the mutation of the gene encoding *Myosin Va*, which is also the cause of neurological diseases like Griscelli syndrome type1 and Elejalde syndrome in humans. In our cerebellar network, the same alteration was reproduced by decreasing the parameter LTD_1 that regulated LTD at the PF-PC plasticity site. Different amounts of damage have been tested, from 10% to 80% of the reference value in physiological conditions. The protocol consisted of one acquisition session including 10 blocks of 10 trials, with 9 CS-US and one CS alone repetitions, CS = 350 ms and US = 100 ms with ISI = 250 ms. We analyzed alterations in adaptation and timing of responses and the modified underlying mechanisms. As for previous cases, we evaluated the performance on a longer acquisition of 1000 trials, in order to verify whether in case of a severe damage to cortical LTD, learning was only delayed or completely compromised.

3. RESULTS

3.1. *Cerebellar model and optimization*

After 100 generations without improvement of the maximum fitness, the optimal parameters were obtained as the mean value of the genes of all the 1-fitness individuals (Table 2). The resulting model achieved an appropriate physiological performance during both acquisition and extinction of the two sessions and an acceptable number of trials with 100% CRs, resulting in a fitness value of 1. The distribution of genes throughout the whole evolution process demonstrated the robustness of the algorithm in exploring the whole search space, while exploiting the best regions (Fig. 2). Multiple good solutions were found, so the final genes were chosen in an intermediate region among near-optimal areas, which mostly corresponded to the convergence regions of the best values for each gene.

To verify the proper behavior of the model with the final parameters, we computed the %CR on a moving window of 10 trials. The obtained fitness value was 1, as acquisition and extinction were achieved within a physiological number of trials; moreover cortical plasticity was responsible for fast learning and nuclear plasticity acted on a slower time scale, matching recent neurophysiological hypotheses[56], and thus demonstrating the proper functioning of the model. The same results were obtained through the EBCC simulations with a shorter ISI, proving the robustness of the final parameters.

3.2. *Loss of Purkinje cells*

The results of PC loss simulations were compared to the reference outcome of experiments on ataxic patients with cerebellar cortical degeneration, suffering a decrease of cerebellar cortical volume of about 20%.[23] We showed that for a small lesion (up to 9 removed PCs, i.e. 12% of all PCs), conditioning occurred as in healthy model (about 80 #CR) and the whole network was able to compensate for the damage (Fig. 3A). When the lesion was more extensive, learning was proportionally compromised, rapidly reaching null %CR. In particular, when removing 15 PCs (i.e. 20% of all PCs), the mean number of total CRs all over the acquisition sequence was 9, which properly matches the corresponding value in the reference study. For this case, we compared the %CR during acquisition to the physiological and the intermediate case with a 16% lesion (Fig. 3B). We showed that the model with 20% PCs removed was able to reproduce the same impaired behavior as in patients: no conditioning occurred and about 10% of CRs was produced starting from the 3rd block. Along acquisition trials, there was not any improvement of %CR, resulting in a final value in the 10th block not significantly different from the values in the initial blocks. Also the timing of simulated responses in case of 20% PC lesion reproduced the alterations in patients: CRs started sooner after the CS onset, resulting in a shortened onset and peak latency (higher absolute values), if compared to normal simulated conditions (Fig. 3C). Specifically, the Wilcoxon-Mann-Whitney test showed differences between healthy and pathological latencies with $p < 0.01$. We analyzed the low-level activity of the network to infer the neural alterations leading to the observed impaired behavior.

Table 2. Genes of the final chosen individual, resulting from the mean of all the 1-fitness individuals.

LTP_1	LTD_1	LTP_2	LTD_2	LTP_3	LTD_3	PF-PC_0	MF-DCN_0	PC-DCN_0
2.09e-2	-4.97e-1	4.44e-7	-3.78e-8	3.65e-7	-3.01e-8	1.46	2.96e-2	3.71e-1

First, we showed that in case of PC loss, the *DCNoutput* of the model was altered in terms of amplitude and shape (Fig. 3D). In fact, as demonstrated by experimental data on animals[32], a damage to PCs causes an improper inhibition on DCNs, which are allowed to fire independently from the IO signal. Therefore, the resulting response during an associative paradigm is not time-locked and learning is compromised. Our model accurately reproduced this

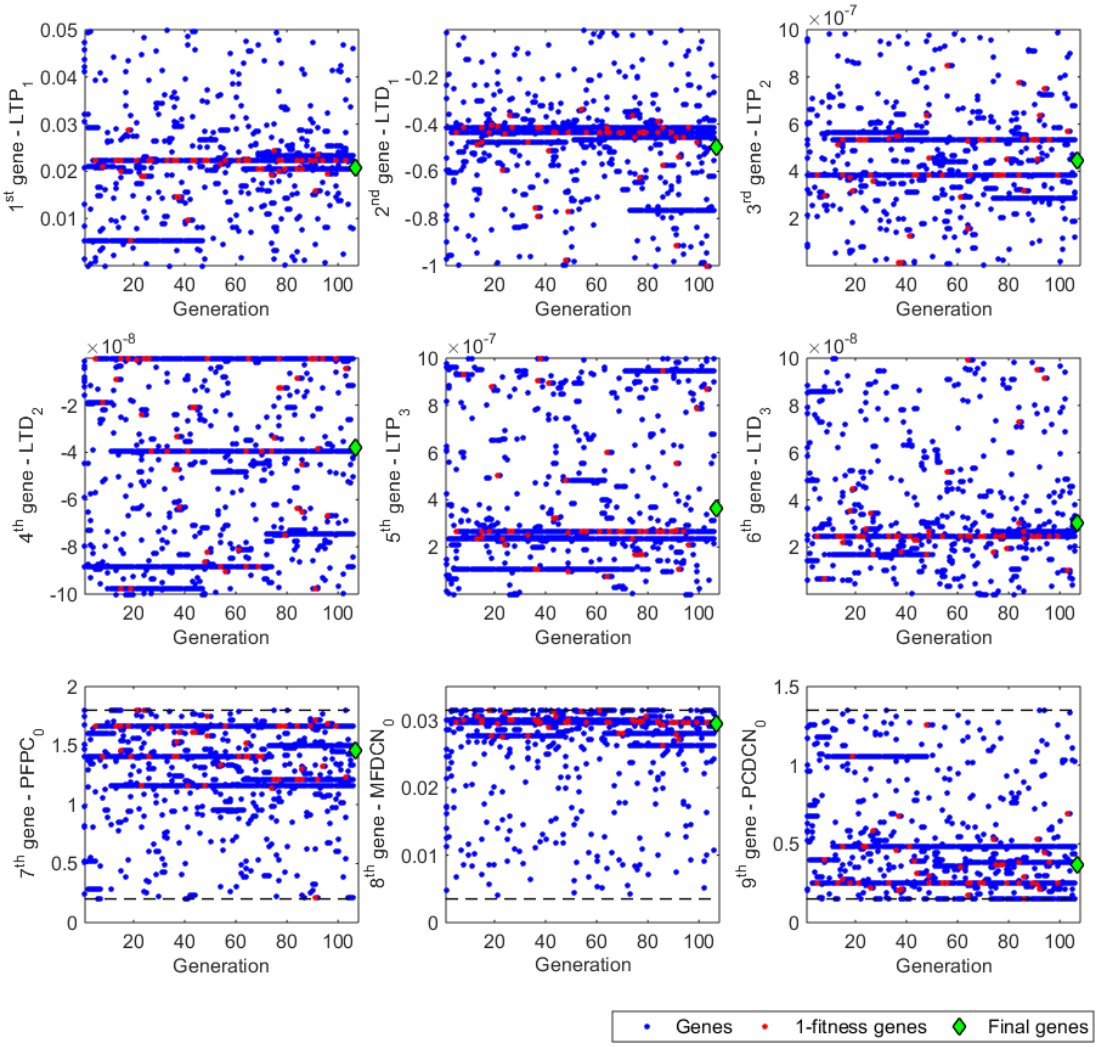

Fig. 2. Distribution of genes along generations. Red dots highlight the values of the 1-fitness genes. At the end of evolution, the green diamonds represent the final optimized parameters for the model.

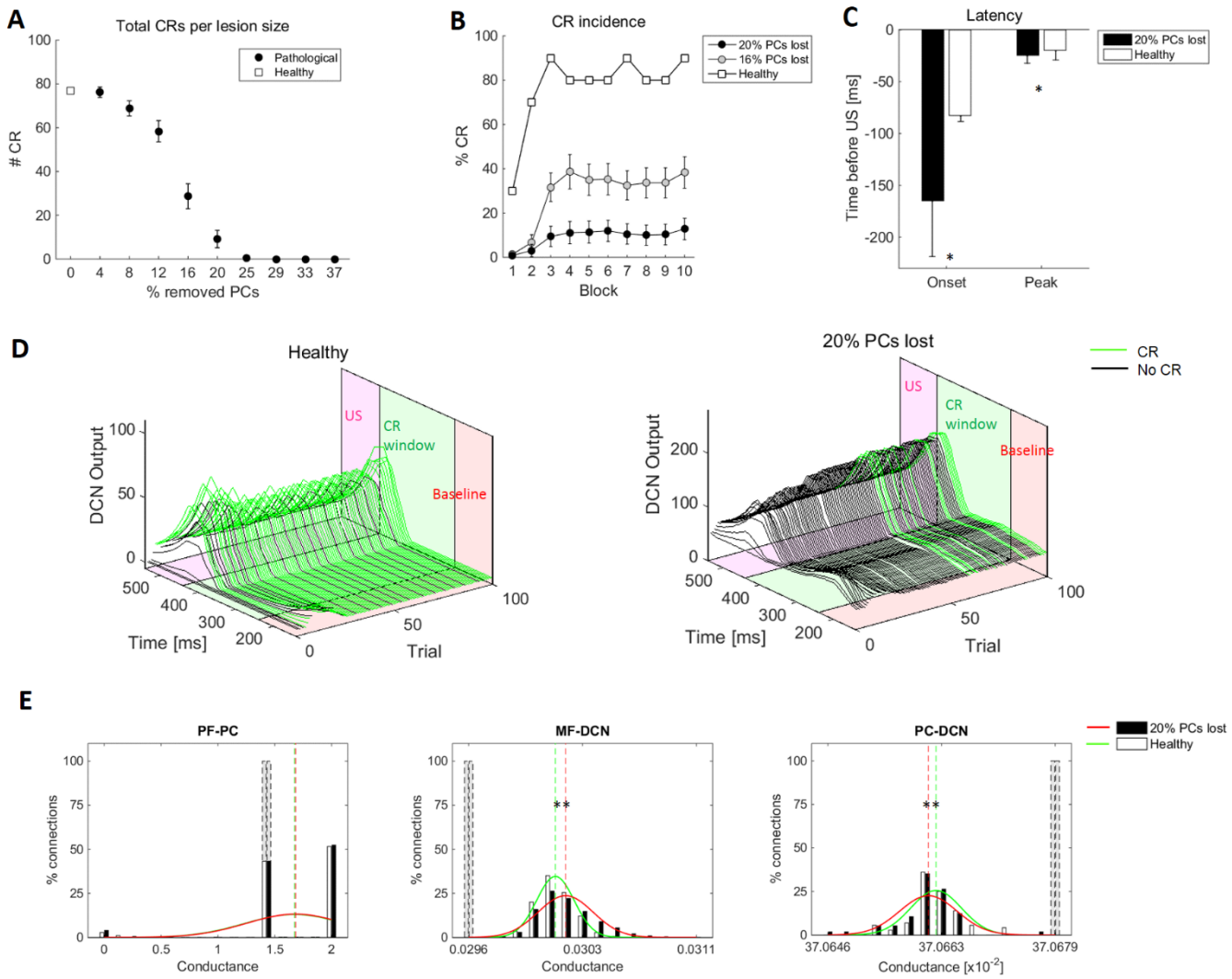

Fig. 3. PC loss. (A) Number of CRs with different amounts of lesion. (B) %CR in case of intermediate and severe damage compared to healthy behavior. (C) Onset and peak latency in case of severe damage, compared to healthy conditions. (D) Cerebellar output throughout the protocol; green lines highlight the trials with CR. (E) Histograms (gray bars for the initial weights; black bars for pathological and white bars for healthy conditions at the end of simulations) of weights for the 3 plasticity sites. Red and green curves are the normal distributions corresponding to the histograms and ** indicates a difference higher than 1% of the full range between pathological and physiological weights.

misbehavior: PC loss resulted in an extended lack of inhibition on DCNs all over the trial; the baseline activity of DCNs increased and the peak in the CR window was not significant to generate a CR (Fig 3D). This low-level damage caused the missed conditioning and the alterations of CRs onset and peak latencies that were previously described. We then analyzed the evolution of synaptic weights to shed light on the modifications of neural plasticity. For both healthy and pathological simulations, we represented the histograms of weights in the three plasticity sites at the beginning and the end of acquisition (Fig. 3E). We showed that the learning mechanism at cortical level was not impaired since the weights reached the same minimum and maximum values as in healthy conditioning. On the other hand, nuclear plasticity proceeded to compensate for the damage: a portion of the MF-DCN weights reached higher values in the pathological case, whereas a part of the PC-DCN conductances decreased to lower values than in physiological simulations. They corresponded to the

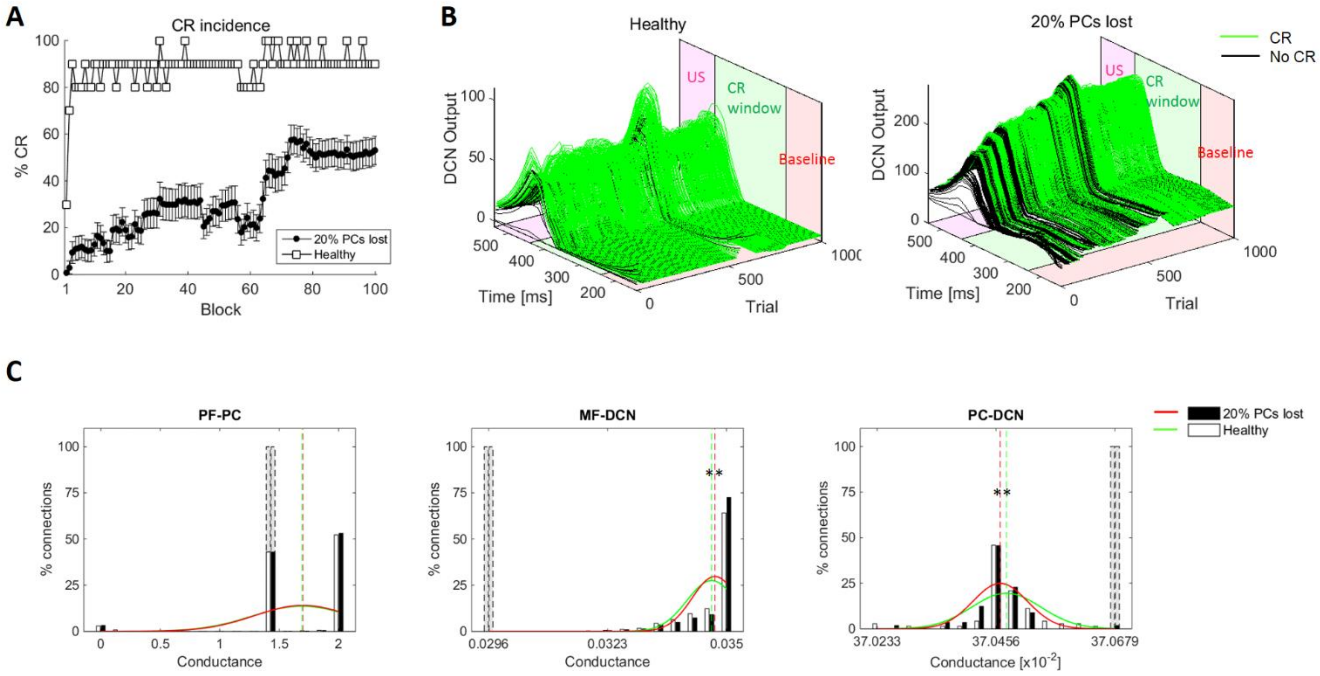

Fig. 4. Long acquisition with 20% PC loss. (A) %CR on blocks of 10 trials for healthy and pathological conditions. (B) Cerebellar output for the healthy (on the left) and the pathological (on the right) model, during the long acquisition protocol; green lines highlight the trials with CR. (C) Histograms (gray bars for the initial weights; black bars for pathological and white bars for healthy conditions at the end of simulations) of weights for the 3 plasticity sites. Red and green curves are the normal distributions corresponding to the histograms and ** indicates a difference higher than 1% of the full range between pathological and physiological weights.

DCNs supposed to generate the CRs and they contributed to increase the output only in the CR time window.

In the long acquisition simulations with 1000 trials, also the pathological model with 20% PC loss succeeded in reaching a higher value of %CR, even if the global performance was poorer and slower than in physiological conditions (Fig. 4A). The evolution of nuclear weights partially compensated for the cortical damage (Fig. 4C), exciting the DCNs in the CR window so as to reach the threshold value, despite the higher *baseline* (Fig. 4B).

3.3. *Impaired cerebellar afferents*

The simulated damage to cerebellar afferents produced a similar behavior both with decreased number of active MFs and with reduced MF firing rate.

The input impairment strongly compromised learning: the mean number of generated CRs dropped below 40 along the 100 acquisition trials from 10% of MF lesion onwards (Fig. 5A). The reference experimental study showed that a damage to Pontine areas caused a decrease of total CR number to 6 within 100 acquisition trials. Starting from this behavioral observation without any quantitative reference about the amount of the damaged area, we used our model to associate a damage extent to the misbehavior; it came out that about 25% of impaired MFs account for the misbehavior, by modeling the impairment both as MF removal and as decreased frequency. Given the similarity of the results, we focused on the model embedding the decreased MF frequency; then, we deepened also the time evolution of %CR along the whole session with 25% damage, comparing it with physiological and an intermediate mild damage (Fig. 5B): no conditioning occurred and there was no improvement of the %CR in late acquisition, similarly to the experimental results on the patient. We computed the onset and peak latency for both physiological and pathological simulated data (Fig. 5C), showing that they were significantly different between the two groups (Wilcoxon-Mann-Whitney test, with $p < 0.01$).

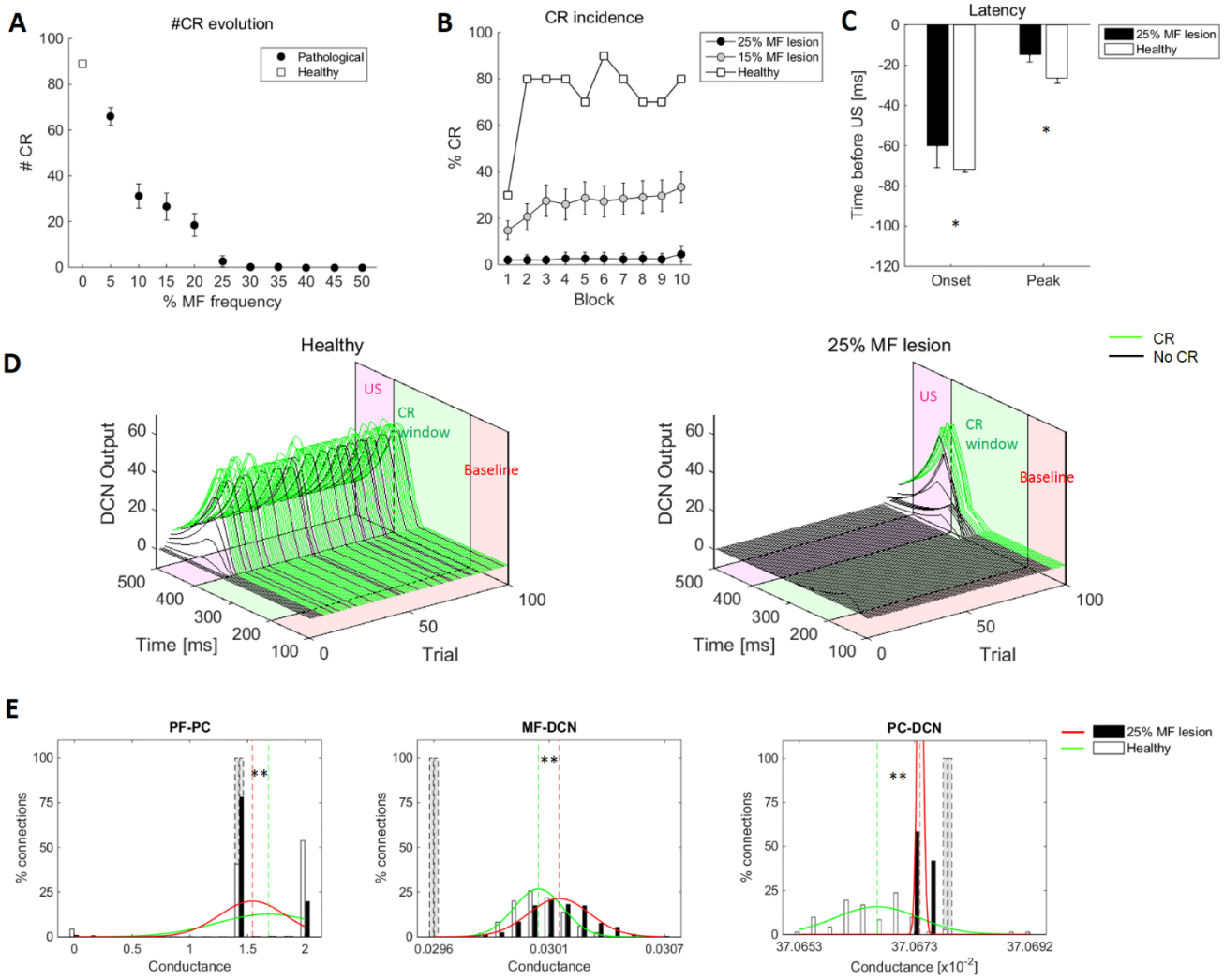

Fig. 5. MF damage. (A) Number of CRs with different amounts of lesion. (B) %CR in case of intermediate and severe damage compared to healthy behavior. (C) Onset and peak latency in case of severe damage, compared to healthy conditions. (D) Cerebellar output throughout the protocol; green lines highlight the trials with CR. (E) Histograms (gray bars for the initial weights; black bars for pathological and white bars for healthy conditions) of weights for the 3 plasticity sites. Red and green curves are the normal distributions corresponding to the histograms and ** indicates a difference higher than 1% of the full range between pathological and physiological weights.

We supposed that the low-level explanation for the altered behavior is that an impaired input on MFs result in a lower excitation on DCNs and a bad encoding in the Granular Layer, which also causes impaired activity of PCs. Indeed, in our simulations the *DCNoutput* was mainly absent (Fig. 5D), because the DCNs received low excitation from MFs and inaccurate inhibition from PCs.

The analysis of synaptic weights (Fig. 5E) demonstrated that learning in the cortex occurred similarly to physiological conditions: some final weights reached zero and others maximum value, but most of weights remained at their initial value, because the corresponding PF-PC synapses were not recruited for learning. On the other hand, in the nuclear sites, PC-DCN weights decreased less in the pathological case if compared to the physiological case; effectively, the proper functioning of this plasticity site requires synchronized spikes of PCs and DCNs, but a damage to MFs caused decreased activity of

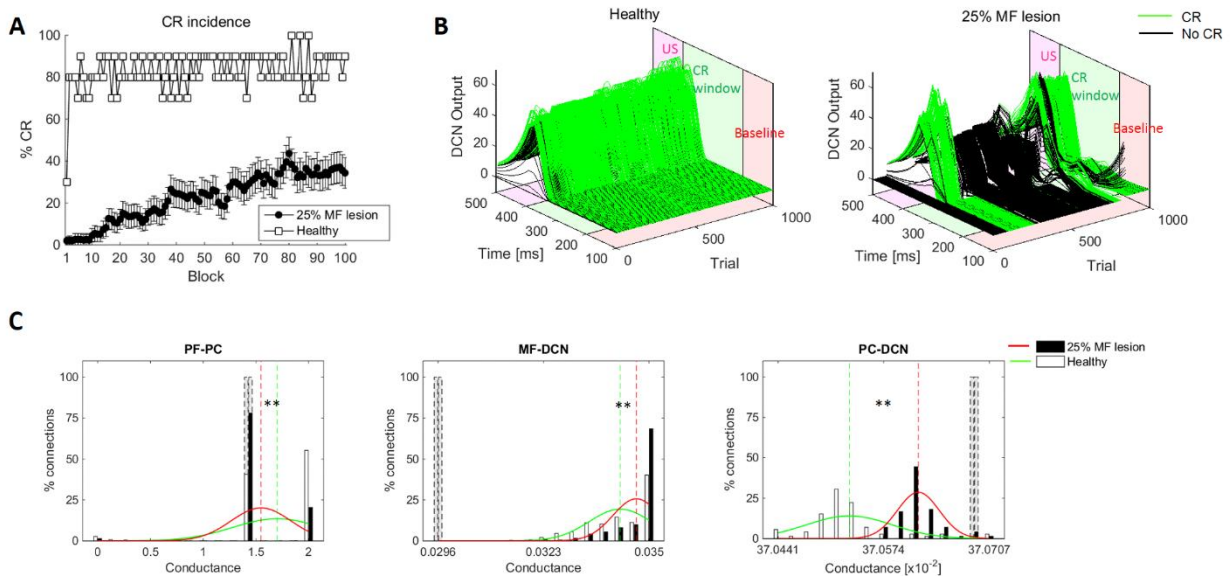

Fig. 6. Long acquisition in case of 25% MF damage. (A) %CR on 100 blocks of 10 trials for healthy and pathological conditions. (B) Cerebellar output for the healthy (on the left) and the pathological (on the right) model, during the long acquisition protocol; green lines highlight the trials with CR. (C) Histograms of weights at the beginning and end of the long acquisition with 25% MF damage. Red and green curves are the normal distributions corresponding to the histograms and ** indicates a difference higher than 1% of the full range between pathological and physiological weights.

both these neural populations. However MF-DCN plasticity allowed to partially obviate the severe damage and to produce some CRs in late acquisition: in fact, the MF-DCN weights were higher than in the healthy case, contributing to increase excitation from MFs on DCNs in the CR window, in order to produce the proper output.

A slight increase of %CR in the last block of acquisition with 25% MF damage (Fig. 5B) and the trend

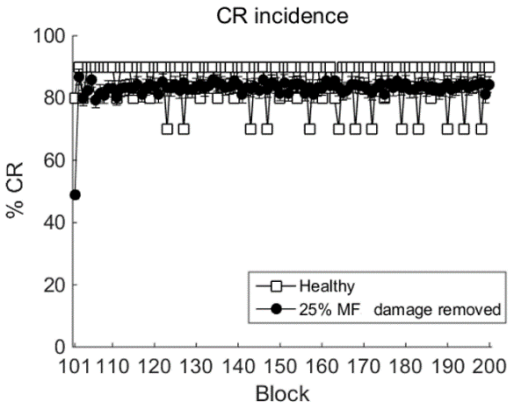

Fig. 7. %CR on 100 blocks of 10 trials, with restored MF physiological activity, after the long acquisition phase with impaired MFs.

of the *DCNoutput* in late acquisition (Fig. 5D) could suggest that learning was not completely compromised but only severely delayed, as hypothesized in the reference study. Along 1000 trials, a slow partial conditioning occurred, with a %CR increase up to 40% (Fig. 6A). The *DCNoutput* started to increase in the CR window on a longer time scale and the result was a stable CR generation in late trials (Fig. 6B). The analysis of weights demonstrated that in the cortical plasticity site a longer acquisition did not suffice to recruit the same amount of PF-PC synapses as in healthy conditions. However, in the nuclear sites a long training caused a significant increase of the MF-DCN weights that was crucial for the generation of CRs and a decrease of PC-DCN weights up to a configuration more similar to the healthy case (Fig. 6C). After this long acquisition phase, the simulations with restored MF damage showed that learning was rapidly recovered if MFs were reactivated as in normal conditions: %CR reached the same level as in the healthy case, for the whole 1000-trial protocol (Fig. 7). This result supported the hypothesis that learning capabilities are generated and stored in both the cortical and nuclear pathways. In fact a damage to MFs affected the Granular layer and consequently the cerebellar cortex, but plasticity at MF-DCN synapses allowed to store information about

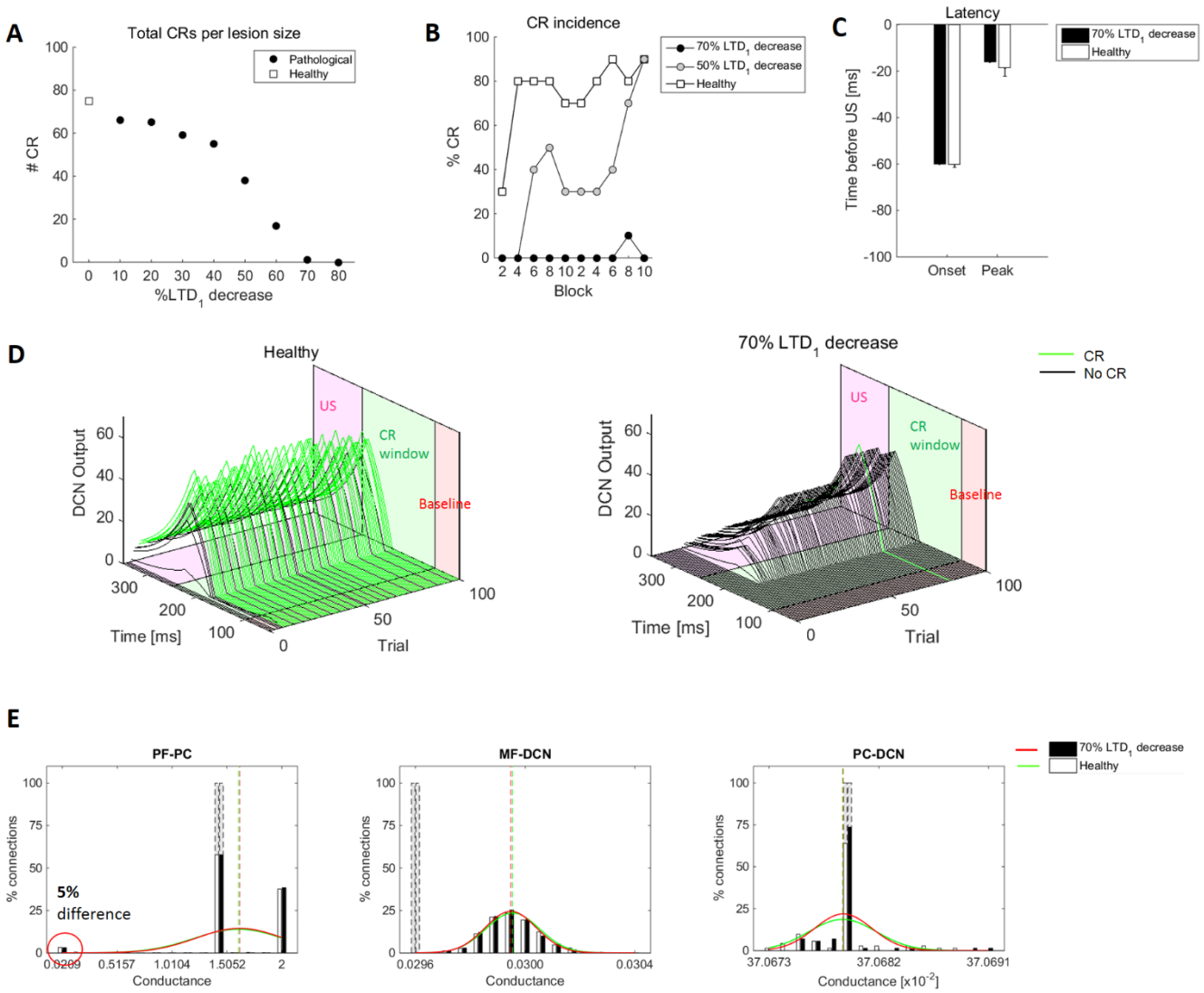

Fig. 8. LTD damage. (A) Number of CRs with different amounts of lesion. (B) %CR in case of intermediate and severe damage compared to healthy behavior. (C) Onset and peak latency in case of severe damage, compared to healthy conditions. (D) Cerebellar output throughout the protocol; green lines highlight the trials with CR. (E) Histograms (gray bars for the initial weights; black bars for pathological and white bars for healthy conditions) of weights for the 3 plasticity sites. The red circle in panel E indicates that there are 5% of the normal LTD weights less in the pathological case.

conditioning on a slow time scale. Therefore, reactivating the normal MF activity after the long acquisition session, learning occurred as in healthy conditions.

3.4. *Impaired LTD at PF-PC synapses*

The simulations of EBCC with impaired LTD at PF-PC connections were inspired by the experimental data from Ref. 25.

First, we focused on the single session of 100 acquisition trials and we analyzed the effects of impaired cortical LTD. The evolution of #CR as the LTD_1 parameter decreased showed that the cerebellum could recover even a high LTD damage, with at least 30 total CRs for LTD_1 reduction up to 50% (Fig. 8A). Moreover, the evaluation of %CR on blocks of 10 trials demonstrated that LTD impairment did not completely compromise learning, but delayed it; for example for an LTD decrease of 50%,

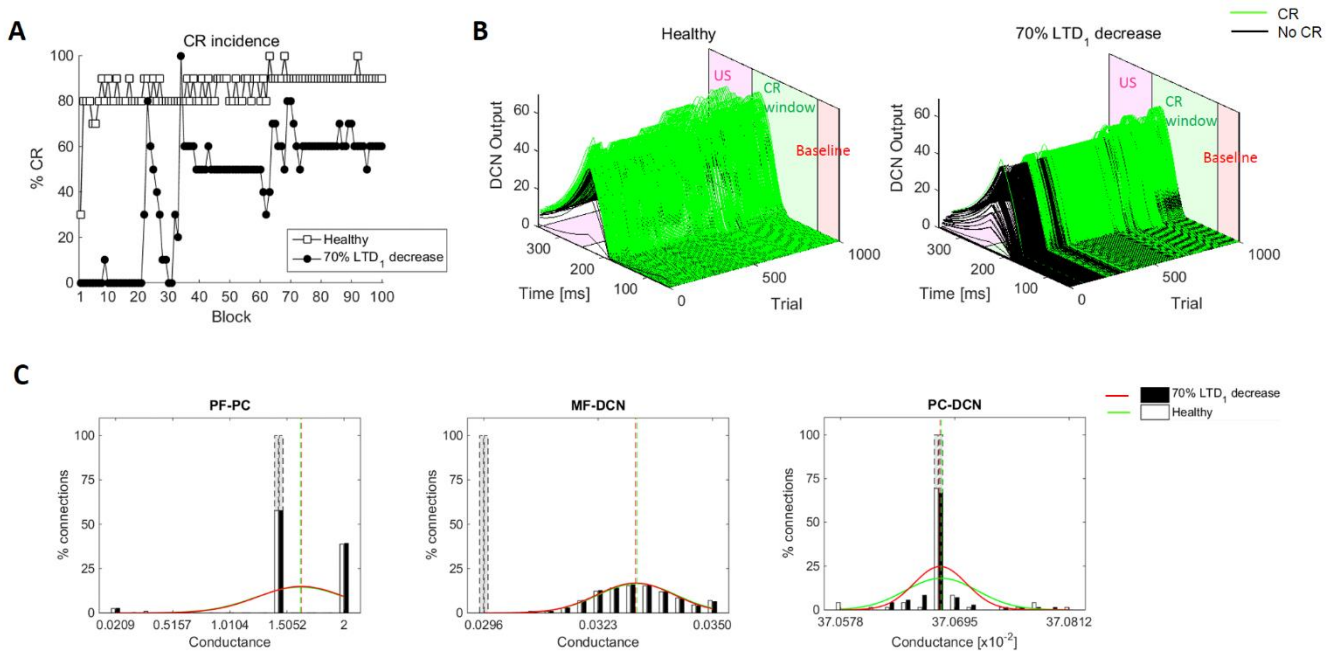

Fig. 9. Long acquisition in case of 70% LTD_1 damage. (A) %CR on 100 blocks of 10 trials. (B) Cerebellar output throughout the protocol, for both healthy and impaired conditions; green lines highlight the trials with CR. (C) Histograms (gray bars for the initial weights; black bars for pathological and white bars for healthy conditions) of weights for the 3 plasticity sites.

healthy values of 80% of CRs were achieved in the late acquisition blocks (Fig. 8B). However, when the LTD_1 lesion overcame a damage of 70% (Fig. 8B) learning was completely switched off, reproducing the same behavior obtained on *dilute-neurological* mutant mice during multiple acquisition sessions. The reduced cortical LTD did not alter the shape of the output (Fig. 8D). Consequently, the timing of CRs was the same as in physiological conditions (Fig. 8C), as demonstrated also by experimental data[25]: for both onset and peak latencies, the Wilcoxon-Mann-Whitney test proved that healthy and pathological values were comparable, with p=0.98 and p=0.20, respectively.

The compromised learning was due only to a slight modification of PF-PC conductances, which were less inhibited than in the healthy case with 5% less weights undergoing LTD in the pathological simulation (Fig. 8E). The damage to LTD_1 also affected the velocity of learning, decreasing the overall DCN activity throughout the acquisition and therefore affected plasticity at PC-DCN connections, which was modeled as STDP triggered by PC and DCN spikes. On the other hand, in the MF-DCN synapses there were not any significant differences between healthy and pathological situations.

On a longer time scale, learning was partially restored (Fig. 9A and 9B), even though %CR did not reach the same level as in the normal case and conditioning was more unstable, because the *DCNoutput* did not have an altered shape, but it did not always verify all the requirements to generate a CR. The evolution of %CR agreed with the results obtained during the multi-session protocol in the reference study.[25] The analysis of weights showed that for all the plasticity sites, the pathological values moved in the same direction as normal values, but the initial differences highlighted in the first session affected even the long protocol (Fig. 9C).

3.5. *Predictions on the changes in neuronal and synaptic activity*

By comparing results in the three cases, it was possible to identify the peculiarities of each pathological condition. During the short acquisition protocol, we obtained a strongly compromised learning, with a decrease of total CRs to less than 12% of the value in healthy conditions. However, the CR timing was differently modified, suggesting different alterations of the underlying neural and synaptic activity. In particular, the values of Δ_i for the

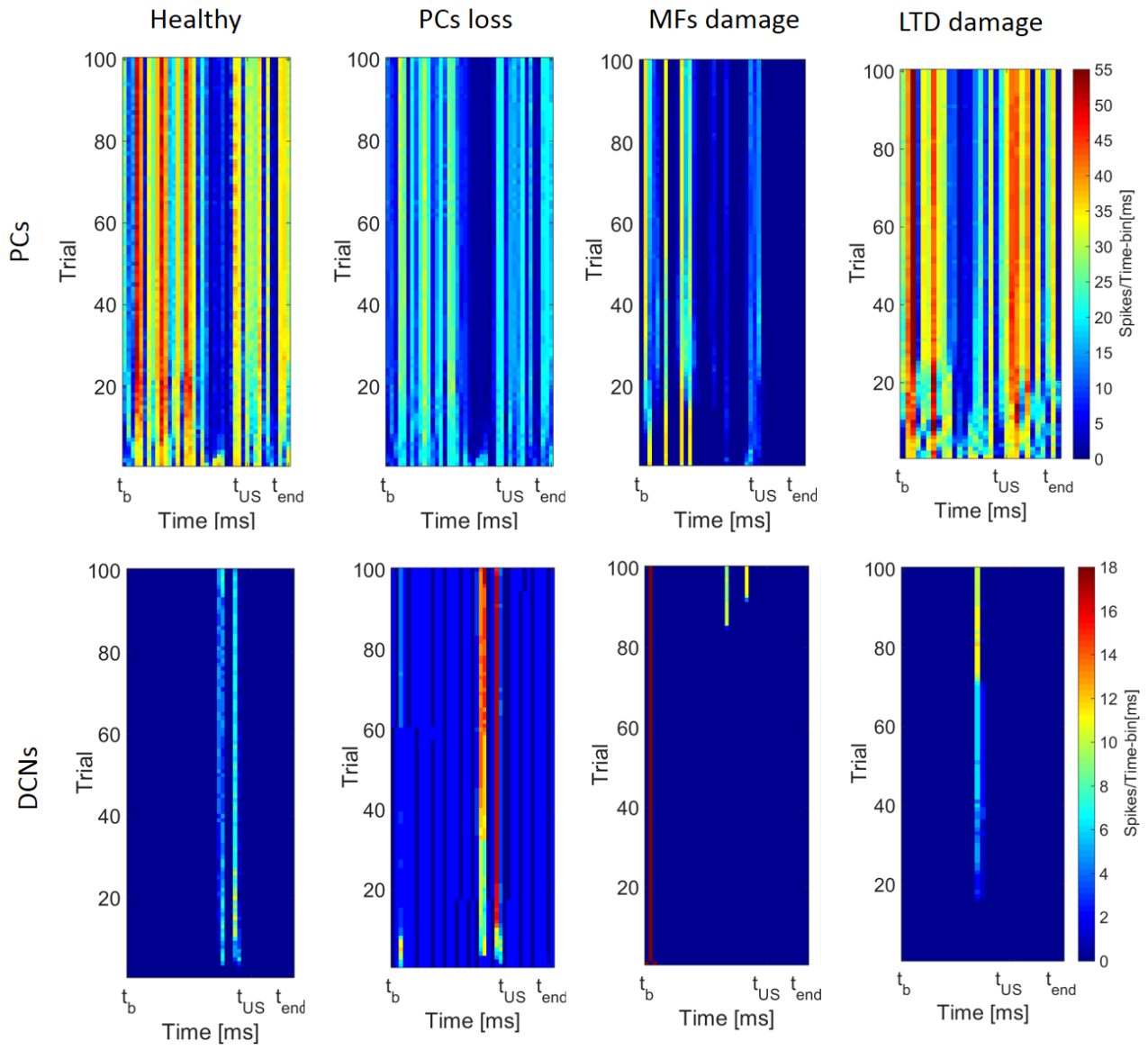

Fig. 10. Firing patterns of PCs (top) and DCNs (bottom) in healthy and pathological conditions: from left to right, healthy, PC loss, MF damage, LTD reduction. For each acquisition trial (vertical dimension), the panels report the number of spikes in time-bins of 10 ms, from t_b (starting of the baseline window) to t_{end} (end of the trial).

three plasticity sites showed how the damages differently impacted on cortical and nuclear learning mechanisms (Table 3).

The representation of firing patterns for PCs and DCNs clearly disclosed the specific features of each case (Fig. 10). During PC loss, the overall activity of PCs was decreased resulting in a lack of inhibition on DCNs, which were allowed to fire through the whole trial duration; thanks to synaptic plasticity, DCN spiking frequency increased in the CR window as acquisition proceeded, but it was not sufficient to differentiate from the high activity at baseline. MF damage resulted in a decreased activity of both PCs and DCNs, without any time-locked variation of frequency; only at late stages of acquisition, DCNs fired in the CR window, as a result of nuclear weight changes. Finally, after cortical LTD reduction, the learning mechanisms were not severely modified as in the previous case, but they were markedly delayed; PC and DCN

activity evolved as in the healthy case, but the neural activity modifications started later (trials 20-30) than in healthy conditions (in which the effects of the learning process appeared after trials 5-10).

Table 3. Summary of pathological simulations outcome. For each type of impairment, we reported the mean #CR and the % of the healthy value (first column), the onset latency as the % of the healthy latency (second column), the parameter Δ_i for each plasticity site (last three columns).

	#CR	Latency	Δ_{PFPC}	Δ_{MFDCN}	Δ_{PCDCN}
PC loss	9 CRs (11.7%)	199%	=	4%	-3%
MF damage	3 CRs (3.4%)	84%	-7%	9%	18%
LTD reduction	1 CR (1.3%)	=	=	=	=

4. DISCUSSION

The aim of this work was to demonstrate that computational models of neural circuits (and biological systems in general) can be a powerful tool not only for testing hypotheses from physiological studies on low-level mechanisms, but also to achieve a deeper insight into pathological conditions. We engaged a realistic cerebellar SNN into the feed-back and feed-forward loops of an entire sensori-motor system operating in closed-loop to associate specific cerebellar microcircuit mechanisms to altered behavioral outcomes. Indeed, the model tunability empowered it with the important property of directly testing hypotheses that associate neuron-scale to behavioral-scale features. This approach demonstrated a high potential not just to investigate the physiological mechanisms of cerebellar control but also to address the mechanisms of various pathological conditions, providing a new powerful tool to understand and act on cerebellar disorders.[21] The simulated behaviors were consistent with experimental observations and, thanks to the realism of the model, it was possible to formulate hypotheses on the low-level mechanisms underlying pathologies and to explore relationships between local lesions and altered behavior. Eventually, the model allowed to quantify low-level parameters and to bind them to the process of plasticity, learning, timing and prediction that characterizes high-level cerebellar control.

4.1. *Specific adaptations differ depending on the underlying network alterations*

The closed-loop simulations reproduced an eye-blink classical conditioning paradigm, in which the number and timing of conditioned responses (CRs) was measured. A comparison of the effect of different pathological changes revealed that, in all cases, CR incidence was strongly reduced compared to healthy conditions (Table 3). Moreover, in all cases, the slow acquisition rate typical of DCN plasticity emerged during the long acquisition protocol. These results were in line with the hypothesis that the cerebellar cortex plays a critical role in fast acquisition of plasticity that is later transferred to DCNs.[48,57,58] In the absence of an effective cerebellar cortex, learning of sensory-motor associations can just proceed at a slow rate and is incomplete. In addition to this common set of changes, adaptation to circuit damage showed characteristic differences among cases: PC loss caused a strong CR delay, MF impairment caused diffused plasticity alterations, LTD decrease caused only minor abnormalities in CR delay and synaptic plasticity.

The differences among these three cases emerged in the firing patterns of PCs and DCNs. Following a PC loss, the basal firing rate of PCs showed a remarkable decrease releasing inappropriate DCN spikes; the CR-related silencing of PCs was very pronounced and triggered an exaggerated DCN time-locked response. Following a MF damage, both PC and DCN activity was severely compromised, so that DCN spikes showed some time-locked spikes only very late during CR acquisition. Following a PF-PC LTD impairment, PC spike suppression was delayed and incomplete, bearing about a late and anomalous increase in DCN activity time-locked to CRs. There are therefore discernible and typical patterns for each kind of lesion, which are further considered in detail below.

4.2. *Loss of Purkinje Cells*

Following PC reduction, the model accurately reproduced the EBCC alterations measured in patients suffering from different types of cerebellar ataxias.[23] A PC loss also characterizes other brain diseases resulting in compromised motor learning. For example, an age-related decrease in the PC number is reported in Alzheimer's disease patients, who also show altered CR generation and timing during EBCC.[40] A PC loss is observed in children with prenatal alcohol exposure, who also show EBCC

alterations.[59] A PC loss associated with motor impairment has been documented in Autism Spectrum Disorders.[60] Therefore, the results obtained here may also be extended to these pathological cases.

Animal experiments have revealed that PC loss is often associated with alterations in other parts of the cerebellar network. In mutant mice with genetically-induced PC loss[61], there is also a decrease in GRs. In mice, prenatal alcohol exposure causes a PC loss and damages to GRs and PF-PC synapses.[62] Although these associated abnormalities may concur to alter the EBCC pattern, the PC is the final common pathway channeling information to DCN, so that reducing the PCs is equivalent to weakening the whole cortical output to DCNs. Indeed, pharmacological blockage of PCs in rabbits caused a higher uniform DCN activity during EBCC, due to the lack of inhibition from the cortex[32,63], which perfectly agrees with the alterations of neural activity in our model. Interestingly, in our simulations the lack of time-locked inhibition of PC on DCN cells was the cause for the modifications in CR timing and rate.

These results confirmed the role of the cerebellar cortex in driving learning on a fast time scale during associative tasks, as predicted by neurophysiological studies.[64] The role of the nuclear pathway in partially compensating for the damage could suggest a key to neurorehabilitation[22]: as the increase of MF-DCN synaptic weights contributed to compensate for the impaired output in our model, an enhanced sensory input to MFs could be used to improve patients recovery.

4.3. *Impaired cerebellar afferents*

There are several forms of ataxia involving structural alterations of the mossy fiber pathways.[65,66] In the case of MF damage, the model was able to reproduce the %CR evolution reported in a reference study on a single cerebellar patient.[24] Consistently, the model predicted that, even after a prolonged training (1000 pairings), conditioning was strongly delayed and weaker than normal. The predicted mechanism was a weaker DCN excitation by MFs and an inaccurate DCN inhibition by PCs. The damage to the cerebellar afferents affected also the Granular Layer, resulting in poor encoding of input signals and reduced plasticity generation. However, the increased action of nuclear plasticity allowed to partially recover the damage and to produce some CRs, though slowly and partially. Although no other EBCC studies are available on patients with impaired cerebellar afferents, we could extend our results to pathologies implying a GR lesion. For example, altered associative learning has been observed in Schizophrenia patients and abnormal activity in the cerebellar Granular layer has been suggested among the causes.[67] Animal experiments also demonstrated the role of a proper input encoding to achieve motor learning: in Ref. 68, they showed that an extensive inactivation of cerebellar GRs prevented from acquisition and consolidation of the Vestibulo-Ocular Reflex (VOR) in mice. They also hypothesized that other plasticity mechanisms could compensate for altered cortical plasticity in case of GR lesion. In particular, a study on EBCC in mice suggested nuclear plasticity as the main compensatory mechanisms when transmission from GRs to PCs was blocked[52], as observed here.

Our work thus supported the hypothesis that nuclear plasticity at MF-DCN connections was responsible for the acquisition of CRs on a long time scale. However, conditioning still remained compromised because the lesions to MFs affected altogether the cortical and nuclear pathways, which are both fundamental for learning. Immediately after restoring the normal MF activity, conditioning occurred as in normal conditions. Thus, our work allowed to identify a redistribution of synaptic plasticity at nuclear sites, suggesting that distributed plastic modifications are fundamental to compensate for damages during pathology.[18,27,56]

4.4. *Impaired LTD at PF-PC synapses*

Further insight into the impact of synaptic plasticity in cerebellar pathology was achieved by simulating a damage in cortical LTD. In such condition, the model was able to reproduce impaired associative learning in mice.[25] CR acquisition was delayed and reduced to a degree depending on the amount of LTD reduction. However, even in case of severe damage, CR acquisition could be at least partially restored over a prolonged acquisition session. Through the representation of synaptic weights we showed that a damage to cortical LTD not only delayed or compromised learning, but also altered nuclear plasticity at PC-DCN synapses. Interestingly, dynamic aspects contributed to compromise nuclear plasticity: plasticity at PC-DCN connections was modeled as STDP, so that a damage to cortical LTD, by delaying PC inhibition, blocked the activity of DCNs required for physiological learning to take place.

Thus, our model supported the neurophysiological hypothesis on the fundamental role of cortical LTD in

driving learning[69], based on the observations that reduced PF-PC synaptic transmission and LTD in genetically modified mice resulted in impaired EBCC. Similar conclusions were achieved in previous experiments[70,71], although other studies questioned the crucial role of cerebellar cortical LTD in motor learning.[72] It should be noted that the absence of major changes in %CR and plasticity redistribution when LTD is decreased can explain why, in mutant mice, disruption of LTD can lead to inconsistent behavioral changes.[56,72,73] Moreover the analysis of neural activity in the model showed that in case of CR, the shape of the output was not modified, thus resulting in the unchanged response timing that matches the experimental findings.

The implications of these modeling results could be extended to other cerebellar pathologies. Indeed, altered LTD (either reduced or enhanced) is associated to specific pathologies, as Autism Spectrum Disorders (ASD)[74] and the Fragile X Syndrome.[75] In particular, the human 15q11-13 duplication, which is typical of ASD, has been studied through a mouse model, showing that the genetic alteration results in reduced cerebellar LTD and altered pruning at CF-PC synapses. Therefore, a more specific computational model of this pathology should include both modifications.

In our simulations of cerebellar plasticity damage, cortical LTD was decreased resulting in reduced CR acquisition without changing CR timing and shape. This case matches the human Griscelli syndrome type I and Elejalde syndrome[25,76], which are characterized by the same *Myosin Va* mutation that caused LTD damage in the reference animal study.[25]

Nevertheless, it should also be noted that we were not able to reproduce the exact experimental protocol during the first 100 trials. This was probably due to the fact that our model was optimized against human data, resulting in a faster conditioning than in mice. This difference suggests that care is needed in comparing animal to human experiments.[77]

4.5. *Advances and limitations of the present study*

Besides the implications for neuropathology, the present work also contributes to validate and update current cerebellar models; in addition to be able to reproduce a variety of physiological behaviors during multiple cerebellum-driven tasks[17,26], these same models turn out now to be able to reproduce pathological states. Actually, closed-loop modeling allowed to simulate dysfunctional behaviors in neuropathological experiments by introducing controlled neural alterations inspired by clinical data.

As a limitation of our study, we imposed a localized damage to the model in order to reproduce prototypical pathological conditions and allow the circuit to activate compensatory effects. This is unusual in real pathological cases, in which the lesion is often distributed over multiple systems, neural populations and cellular mechanisms. However, the possibility to unequivocally isolate the damage is crucial to identify the causes of diseases and the causality of the underlying mechanisms, especially because it cannot easily be achieved in human or animal experiments.

Future work will have to consider more complex paradigms like VOR, and to use more realistic cerebellar and system models, including extracerebellar connections.[78] In particular, within the cerebellar model we will incorporate new neuronal properties like DCN pacemaking, chaotic and stochastic resonance in IOs[79,80], and regulatory circuits like the interneuron inhibitory networks of granular and molecular layer. This would allow a careful analysis of spike patterns in the neuronal populations of the model, providing further hints of the inner structure of network computation and of its alterations in pathology.[81,82] Moreover, the introduction of other plasticity sites would be necessary to better understand the role of synaptic plasticity in compensating for a pathological condition. For example, plasticity at MF-GR connections has been demonstrated by neurophysiological studies[56] and its role could be clarified through the use of a computational model, also in case of cerebellar damages. Plasticity between IOs and DCNs has been predicted to accelerate learning toward biological levels.[83]

It will also be useful to extend modeling to other mechanisms typical of cerebellar diseases: irregular firing patterns of PCs have been recognized in animal models of dystonia[84], and oscillations in the Inferior Olive have been demonstrated in case of Essential Tremor.[85] This more complex role of IOs will make it necessary to introduce dynamic properties in the IO circuit (e.g. oscillation and resonance)[86,87], which have been shown in neurophysiological studies.[88]

4.6. *Conclusions and perspectives*

These closed-loop simulations reproduced several aspects of cerebellar pathologies revealed in human and animal experiments, allowing to predict how the

underlying neural mechanisms operate in normal conditions and during compensation to network damage. The current method may help developing new tools for medicine, by exploiting the bidirectional correspondence between computational and experimental worlds in order to verify new pathogenetic hypotheses and define appropriate corrective strategies. The specific patient's cerebellar microcircuit, inserted into control loops designed ad-hoc to perform behavioral tasks within a real environment, could provide a new tool to model experimental data, to associate and decompose the corresponding underlying mechanisms and to hypothesize modifications induced by neural perturbations or dysfunctions. As a result, it may be envisaged that a new knowledge will be gained on the adaptation mechanisms occurring during brain diseases, which still remain largely unknown. This would allow to move from the static "lesion-symptom" view of diseases, still widely adopted, toward a more sophisticated understanding of the internal circuit dynamics determined by circuit adaptations based on recurrent circuit loops and neural plasticity. The present approach is non-invasive and can help distinguishing among the overwhelming number of possible configurations that the neural system can assume during repair following a lesion. Model simulations could help containing animal experimentation (3Rs principle: Replacement, Reduction and Refinement[89]), which would then be needed to test selected hypotheses rather than explore an immense field of possibilities. This approach may eventually lead to design new diagnostic and therapeutic tools addressing the concepts of personalized medicine in neurorehabilitation.[90–95]

Acknowledgements

The work was supported by grants of the European Union (CEREBNET FP7-ITN238686, REALNET P7-ICT270434, Human Brain Project HBP-604102) and Regione Lombardia (HBP-Lombardia project).

Conflict of interest

The authors declare that they have no conflict of interest.

References

1. J.E. Steinmetz and D.R. Sengelaub, Possible conditioned stimulus pathway for classical eyelid conditioning in rabbits. I. Anatomical evidence for direct projections from the pontine nuclei to the cerebellar interpositus nucleus, *Behav. Neural Biol.* **57**(2) (1992) 103–115.
2. G. Crabtree and J.A. Gogos, Synaptic plasticity, neural circuits and the emerging role of altered short-term information processing in schizophrenia, *Front. Synaptic Neurosci.* **6**(28) (2014) 1–27.
3. M. Ito, Cerebellar circuitry as a neuronal machine, *Prog. Neurobiol.* **78**(3–5) (2006) 272–303.
4. M. Ito, Error detection and representation in the olivo-cerebellar system, *Front. Neural Circuits* **7**(1) (2013) 1–8.
5. M. Ito, K. Yamaguchi, S. Nagao and T. Yamazaki, Long-term depression as a model of cerebellar plasticity, *Prog. Brain Res.* **210** (2014) 1–30.
6. E. D'Angelo and S. Casali, Seeking a unified framework for cerebellar function and dysfunction: from circuit operations to cognition, *Front. Neural Circuits* **6**(116) (2013) 1–23.
7. E. D'Angelo, S. Solinas, J.A. Garrido, C. Casellato, A. Pedrocchi, J. Mapelli, D. Gandolfi and F. Prestori, Realistic modeling of neurons and networks: towards brain simulation, *Funct. Neurol.* **28**(3) (2013) 153–166.
8. E. D'Angelo, L. Mapelli, C. Casellato, J.A. Garrido, N. Luque, J. Monaco, F. Prestori, A. Pedrocchi and E. Ros, Distributed Circuit Plasticity: New Clues for the Cerebellar Mechanisms of Learning, *The Cerebellum* **15** (2016) 139–151.
9. D. Caligiore, G. Pezzulo, R.C. Miall and G. Baldassarre, The contribution of brain sub-cortical loops in the expression and acquisition of action understanding abilities, *Neurosci. Biobehav. Rev.* **37**(10) (2013) 2504–2515.
10. D. Caligiore, G. Pezzulo, G. Baldassarre, A.C. Bostan, P.L. Strick, K. Doya, R.C. Helmich, M. Dirkx, J. Houk, H. Jörntell, A. Lago-Rodriguez, J.M. Galea, R.C. Miall, T. Popa, A. Kishore, P.F.M.J. Verschure, R. Zucca and I. Herreros, Consensus Paper: Towards a Systems-Level View of Cerebellar Function: the Interplay Between Cerebellum, Basal Ganglia, and Cortex, *The Cerebellum* (2016) .
11. J.F. Medina, W.L. Nores, T. Ohyama and M.D. Mauk, Mechanisms of cerebellar learning suggested by eyelid conditioning, *Curr. Opin. Neurobiol.* **10**(6) (2000) 717–724.
12. S. Ghosh-Dastidar and H. Adeli, Spiking Neural Networks, *Int. J. Neural Syst.* **19**(4) (2009) 295–308.
13. S. Ghosh-Dastidar and H. Adeli, *Third Generation Neural Networks: Spiking Neural Networks*, in *Advances in Computational Intelligence* (2009), pp. 167–178.
14. S. Ghosh-Dastidar and H. Adeli, A new supervised

learning algorithm for multiple spiking neural networks with application in epilepsy and seizure detection, *Neural Networks* **22**(10) (2009) 1419–1431.
15. S. Ghosh-Dastidar and H. Adeli, Improved Spiking Neural Networks for EEG Classification and Epilepsy and Seizure Detection, *Integr. Comput. Aided. Eng.* **14**(3) (2007) 187–212.
16. H. Adeli and S. Ghosh-Dastidar, *Automated EEG-based Diagnosis of Neurological Disorders - Inventing the Future of Neurology*, (CRC Press, Taylor & Francis, 2010).
17. A. Antonietti, C. Casellato, J.A. Garrido, E. D'Angelo and A. Pedrocchi, Spiking cerebellar model with multiple plasticity sites reproduces eye blinking classical conditioning, in *International IEEE/EMBS Conference on Neural Engineering, NER* (2015), pp. 296–299.
18. A. Antonietti, C. Casellato, J.A. Garrido, N.R. Luque, F. Naveros, E. Ros, E. D'Angelo and A. Pedrocchi, Spiking Neural Network With Distributed Plasticity Reproduces Cerebellar Learning in Eye Blink Conditioning Paradigms, *IEEE Trans. Biomed. Eng.* **63**(1) (2016) 210–9.
19. A. Antonietti, C. Casellato, A. Geminiani, E. D'Angelo and A. Pedrocchi, Healthy and Pathological Cerebellar Spiking Neural Networks in Vestibulo-Ocular Reflex, in *Engineering in Medicine and Biology Society (EMBC), 2015 37th Annual International Conference of the IEEE* (2015), pp. 2514–2517.
20. A. Geminiani, A. Antonietti, C. Casellato, E. D'Angelo and A. Pedrocchi, A Computational Model of the Cerebellum to Simulate Cortical Degeneration During a Pavlovian Associative Paradigm, in *IFBME Proceedings on the XIV Mediterranean Conference on Medical and Biological Engineering and Computing* (2016), pp. 1063–1068.
21. H. Markram, Seven challenges for neuroscience, *Funct. Neurol.* **28**(3) (2013) 145–151.
22. W. Ilg and D. Timmann, *General Management of Cerebellar Disorders: an Overview*, in *Handbook of the Cerebellum and Cerebellar Disorders* (2013), pp. 2349–2368.
23. A. Dimitrova, M. Gerwig, B. Brol, E.R. Gizewski, M. Forsting, A. Beck, V. Aurich, F.P. Kolb and D. Timmann, Correlation of cerebellar volume with eyeblink conditioning in healthy subjects and in patients with cerebellar cortical degeneration, *Brain Res.* **1198** (2008) 73–84.
24. P.R. Solomon, G.T. Stowe and W.W. Pendlbeury, Disrupted eyelid conditioning in a patient with damage to cerebellar afferents, *Behav. Neurosci.* **103**(4) (1989) 898–902.
25. M. Miyata, Y. Kishimoto, M. Tanaka, K. Hashimoto, N. Hirashima, Y. Murata, M. Kano and Y. Takagishi, A Role for Myosin Va in Cerebellar Plasticity and Motor Learning: A Possible Mechanism Underlying Neurological Disorder in Myosin Va Disease, *J. Neurosci.* **31**(16) (2011) 6067–6078.
26. C. Casellato, A. Antonietti, J.A. Garrido, R.R. Carrillo, N.R. Luque, E. Ros, A. Pedrocchi and E. D'Angelo, Adaptive robotic control driven by a versatile spiking cerebellar network, *PLoS One* **9**(11) (2014) 1–17.
27. C. Casellato, A. Antonietti, J.A. Garrido, G. Ferrigno, E. D'Angelo and A. Pedrocchi, Distributed cerebellar plasticity implements generalized multiple-scale memory components in real-robot sensorimotor tasks, *Front. Comput. Neurosci.* **9**(24) (2015) 1–14.
28. E. Ros, R. Carrillo, E.M. Ortigosa, B. Barbour and R. Agís, Event-driven simulation scheme for spiking neural networks using lookup tables to characterize neuronal dynamics, *Neural Comput.* **18**(12) (2006) 2959–2993.
29. R.R. Carrillo, E. Ros, B. Barbour, C. Boucheny and O. Coenen, Event-driven simulation of neural population synchronization facilitated by electrical coupling, *BioSystems* **87** (2007) 275–280.
30. R.R. Carrillo, E. Ros, C. Boucheny and O.J.M.D. Coenen, A real-time spiking cerebellum model for learning robot control, *BioSystems* **94** (2008) 18–27.
31. T. Yamazaki and S. Tanaka, The cerebellum as a liquid state machine, *Neural Networks* **20**(3) (2007) 290–297.
32. J.F. Medina, K.S. Garcia, W.L. Nores, N.M. Taylor and M.D. Mauk, Timing mechanisms in the cerebellum: testing predictions of a large-scale computer simulation, *J. Neurosci.* **20**(14) (2000) 5516–5525.
33. Z. Wang, L. Guo and M. Adjouadi, A Generalized Leaky Integrate-and-Fire Neuron Model With Fast Implementation Method, *Int. J. Neural Syst.* **24**(5) (2014) .
34. E. D'Angelo, G. De Filippi, P. Rossi, V. Taglietti, F. Generale and V. Forlanini, Synaptic excitation of individual rat cerebellar granule cells in situ : evidence for the role of NMDA receptors, *J. Physiol.* **484**(2) (1995) 397–413.
35. R. Maex and E. De Schutter, Synchronization of Golgi and Granule Cell Firing in a Detailed Network Model of the Cerebellar Granule Cell Layer Synchronization of Golgi and Granule Cell Firing in a Detailed Network Model of the Cerebellar Granule Cell Layer, *J. Neurophysiol.* **80** (2013) 2521–2537.
36. S. Solinas, R. Maex and E. De Schutter, Synchronization of Purkinje cell pairs along the parallel fiber axis: A model, *Neurocomputing* **52**–**54** (2003) 97–102.
37. S. Brandi, I. Herreros and P.F.M.J. Verschure, *Optimization of the anticipatory reflexes of a computational model of the cerebellum*, in *Biomimetic and Biohybrid Systems* (Springer International Publishing, 2014), pp. 11–22.
38. I. Herreros and P.F.M.J. Verschure, Nucleo-olivary inhibition balances the interaction between the reactive and

adaptive layers in motor control, *Neural Networks* **47** (2013) 64–71.

39. I. Herreros, G. Maffei, S. Brandi, M. Sanchez-Fibla and P.F.M.J. Verschure, Speed generalization capabilities of a cerebellar model on a rapid navigation task, in *IEEE/RSJ International Conference on Intelligent Robots and Systems (IROS)* (2013), pp. 363–368.
40. D.S. Woodruff-Pak, M. Papka, S. Romano and Y.-T. Li, Eyeblink Classical Conditioning in Alzheimer' s Disease and Cerebrovascular Dementia, *Neurobiol. Aging* **17**(4) (1996) 505–512.
41. D. Timmann, M. Gerwig, M. Frings, M. Maschke and F.P. Kolb, Eyeblink conditioning in patients with hereditary ataxia: A one-year follow-up study, *Exp. Brain Res.* **162** (2005) 332–345.
42. K.L. Parker, N.C. Andreasen, D. Liu, J.H. Freeman, L.L. Boles Ponto and D.S. O'Leary, Eyeblink Conditioning in Healthy Adults: A Positron Emission Tomography Study, *The Cerebellum* **11**(4) (2012) 1–18.
43. M. Gerwig, A. Dimitrova, F.P. Kolb, M. Maschke, B. Brol, A. Kunnel, D. Boring, A.F. Thilmann, M. Forsting, H.C. Diener and D. Timmann, Comparison of eyeblink conditioning in patients with superior and posterior inferior cerebellar lesions, *Brain* **126** (2003) 71–94.
44. M. Gerwig, K. Hajjar, A. Dimitrova, M. Maschke, F.P. Kolb, M. Frings, A.F. Thilmann, M. Forsting, H.C. Diener and D. Timmann, Timing of Conditioned Eyeblink Responses Is Impaired in Cerebellar Patients, *J. Neurosci.* **25**(15) (2005) 3919–3931.
45. H. Adeli and S.-L. Hung, *Machine learning: neural networks, genetic algorithms, and fuzzy systems*, (John Wiley & Sons, 1994).
46. K.D. Carlson, J.M. Nageswaran, N. Dutt and J.L. Krichmar, An efficient automated parameter tuning framework for spiking neural networks, *Front. Neurosci.* **8**(10) (2014) 1–15.
47. V. Bracha, L. Zhao, K.B. Irwin and J.R. Bloedel, The human cerebellum and associative learning: dissociation between the acquisition, retention and extinction of conditioned eyeblinks, *Brain Res.* **860** (2000) 87–94.
48. J. Monaco, C. Casellato, G. Koch and E. D'Angelo, Cerebellar theta burst stimulation dissociates memory components in eyeblink classical conditioning, *Eur. J. Neurosci.* **40** (2014) 3363–3370.
49. D.-A. Jirenhed, F. Bengtsson and G. Hesslow, Acquisition, extinction, and reacquisition of a cerebellar cortical memory trace, *J. Neurosci.* **27**(10) (2007) 2493–502.
50. S. Toru, T. Murakoshi, K. Ishikawa, H. Saegusa, H. Fujigasaki, T. Uchihara, S. Nagayama, M. Osanai, H. Mizusawa and T. Tanabe, Spinocerebellar Ataxia Type 6 Mutation Alters P-type Calcium Channel Function, *J. Biol. Chem.* **275**(15) (2000) 10893–10898.
51. S.W. Jacobson, M.E. Stanton, N.C. Dodge, M. Pienaar, D.S. Fuller, C.D. Molteno, E.M. Meintjes, H.E. Hoyme, L.K. Robinson, N. Khaole and J.L. Jacobson, Impaired Delay and Trace Eyeblink Conditioning in School-Age Children With Fetal Alcohol Syndrome, *Alcohol. Clin. Exp. Res.* **35**(2) (2011) 250–264.
52. N. Wada, Y. Kishimoto, D. Watanabe, M. Kano, T. Hirano, K. Funabiki and S. Nakanishi, Conditioned eyeblink learning is formed and stored without cerebellar granule cell transmission, *Proc. Natl. Acad. Sci. U. S. A.* **104**(42) (2007) 16690–5.
53. C.I. De Zeeuw, C. Hansel, F. Bian, S.K.E. Koekkoek, A.M. van Alphen, D.J. Linden and J. Oberdick, Expression of a protein kinase C inhibitor in Purkinje cells blocks cerebellar LTD and adaptation of the vestibulo-ocular reflex, *Neuron* **20** (1998) 495–508.
54. W. Kakegawa, T. Miyazaki, K. Emi, K. Matsuda, K. Kohda, J. Motohashi, M. Mishina, S. Kawahara, M. Watanabe and M. Yuzaki, Differential Regulation of Synaptic Plasticity and Cerebellar Motor Learning by the C-Terminal PDZ-Binding Motif of GluRd2, *J. Neurosci.* **28**(6) (2008) 1460–1468.
55. M. Yuzaki, Cerebellar LTD vs. motor learning-Lessons learned from studying GluD2, *Neural Networks* **47** (2013) 36–41.
56. E. D'Angelo, The organization of plasticity in the cerebellar cortex: from synapses to control, *Prog. Brain Res.* **210** (2014) 31–58.
57. R. Shadmehr, M.A. Smith and J.W. Krakauer, Error Correction, Sensory Prediction, and Adaptation in Motor Control, *Annu. Rev. Neurosci.* **33**(1) (2010) 89–108.
58. M.A. Smith, A. Ghazizadeh and R. Shadmehr, Interacting adaptive processes with different timescales underlie short-term motor learning, *PLoS Biol.* **4**(6) (2006) 1035–1043.
59. J.M. Coffin, S. Baroody, K. Schneider and J.O. Neill, Impaired cerebellar learning in children with Prenatal Alcohol Exposure: A comparative study of eyeblink conditioning in children with ADHD and dyslexia, *Cortex* **41**(3) (2005) 389–398.
60. M.W. Mosconi, Z. Wang, L.M. Schmitt, P. Tsai and J.A. Sweeney, The role of cerebellar circuitry alterations in the pathophysiology of autism spectrum disorders, *Front. Neurosci.* **9**(296) (2015) 1–24.
61. Y. Kishimoto, M. Hirono, R. Atarashi, S. Sakaguchi, T. Yoshioka, S. Katamine and Y. Kirino, Age-Dependent Impairment of Eyeblink Conditioning in Prion Protein-Deficient Mice, *PLoS One* **8**(4) (2013) 1–10.
62. D.T. Cheng, S.W. Jacobson, J.L. Jacobson, C.D. Molteno, M.E. Stanton and J.E. Desmond, Eyeblink classical conditioning in alcoholism and fetal alcohol spectrum disorders, *Front. Psychiatry* **6**(155) (2015) 1–7.
63. K.S. Garcia and M.D. Mauk, Pharmacological

analysis of cerebellar contributions to the timing and expression of conditioned eyelid responses, *Neuropharmacology* **37** (1998) 471–480.

64. C.G. Logan and S.T. Grafton, Functional anatomy of human eyeblink conditioning determined with regional cerebral glucose metabolism and positron-emission tomography, *PNAS Proc. Natl. Acad. Sci. United States Am.* **92**(16) (1995) 7500–7504.
65. M. Manto, The wide spectrum of spinocerebellar ataxias (SCAs), *The Cerebellum* **4**(1) (2005) 2–6.
66. M. Manto and D. Marmolino, Cerebellar ataxias, *Curr. Opin. Neurol.* **22**(4) (2009) 419–429.
67. J.K. Forsyth, A.R. Bolbecker, C.S. Mehta, M.J. Klaunig, J.E. Steinmetz, B.F. O'Donnell and W.P. Hetrick, Cerebellar-dependent eyeblink conditioning deficits in schizophrenia spectrum disorders, *Schizophr. Bull.* **38**(4) (2012) 751–759.
68. E. Galliano, Z. Gao, M. Schonewille, B. Todorov, E. Simons, A.S. Pop, E. D'Angelo, A.M.J.M. Van Den Maagdenberg, F.E. Hoebeek and C.I. De Zeeuw, Silencing the Majority of Cerebellar Granule Cells Uncovers Their Essential Role in Motor Learning and Consolidation, *Cell Rep.* **3**(4) (2013) 1239–1251.
69. K. Emi, W. Kakegawa, E. Miura, A. Ito-Ishida, K. Kohda and M. Yuzaki, Reevaluation of the role of parallel fiber synapses in delay eyeblink conditioning in mice using Cbln1 as a tool, *Front. Neural Circuits* **7**(180) (2013) 1–14.
70. K. Shibuki, H. Gomi, L. Chen, S. Bao, J.J. Kim, H. Wakatsuki, T. Fujisaki, K. Fujimoto, A. Katoh, T. Ikeda, C. Chen, R.F. Thompson and S. Itohara, Deficient cerebellar long-term depression, impaired eyeblink conditioning, and normal motor coordination in GFAP mutant mice, *Neuron* **16**(3) (1996) 587–599.
71. A. Belmeguenai, P. Botta, J.T. Weber, M. Carta, M. De Ruiter, C.I. De Zeeuw, C.F. Valenzuela and C. Hansel, Alcohol impairs long-term depression at the cerebellar parallel fiber-Purkinje cell synapse, *J. Neurophysiol.* **100**(6) (2008) 3167–3174.
72. M. Schonewille, Z. Gao, H.J. Boele, M.F. Vinueza Veloz, W.E. Amerika, A.A.M. Simek, M.T. De Jeu, J.P. Steinberg, K. Takamiya, F.E. Hoebeek, D.J. Linden, R.L. Huganir and C.I. De Zeeuw, Reevaluating the Role of LTD in Cerebellar Motor Learning, *Neuron* **70**(1) (2011) 43–50.
73. Z. Gao, B.J. van Beugen and C.I. De Zeeuw, Distributed synergistic plasticity and cerebellar learning, *Nat. Rev. Neurosci.* **13** (2012) 619–635.
74. C. Piochon, A.D. Kloth, G. Grasselli, H.K. Titley, H. Nakayama, K. Hashimoto, V. Wan, D.H. Simmons, T. Eissa, J. Nakatani, A. Cherskov, T. Miyazaki, M. Watanabe, T. Takumi, M. Kano, S.S.-H. Wang and C. Hansel, Cerebellar plasticity and motor learning deficits in a copy-number variation mouse model of autism, *Nat. Commun.* **5** (2014) 5586.
75. S.K.E. Koekkoek, K. Yamaguchi, B.A. Milojkovic, B.R. Dortland, T.J.H. Ruigrok, R. Maex, W. De Graaf, A.E. Smit, F. Vanderwerf, C.E. Bakker, R. Willemsen, T. Ikeda, S. Kakizawa, K. Onodera, D.L. Nelson, E. Mientjes, M. Joosten, E. De Schutter, B.A. Oostra, M. Ito, C.I. De Zeeuw, E. Mc and P.O. Box, Deletion of FMR1 in Purkinje Cells Enhances Parallel Fiber LTD, Enlarges Spines, and Attenuates Cerebellar Eyelid Conditioning in Fragile X Syndrome, *Neuron* **47**(3) (2005) 339–352.
76. R.T. Libby, C. Lillo, J. Kitamoto, D.S. Williams and K.P. Steel, Myosin Va is required for normal photoreceptor synaptic activity, *J. Cell Sci.* **117**(19) (2004) 4509–15.
77. P. McGonigle and B. Ruggeri, Animal models of human disease: Challenges in enabling translation, *Biochem. Pharmacol.* **87** (2014) 162–171.
78. B. Strack, K.M. Jacobs and K.J. Cios, Simulating Vertical and Horizontal Inhibition With Short-Term Dynamics in a Multi-Column Multi-Layer Model of Neocortex, *Int. J. Neural Syst.* **24**(5) (2014) .
79. S. Nobukawa and H. Nishimura, Characteristic of Signal Response in Coupled Inferior Olive Neurons with Velarde-Llinás Model, in *Proceedings of the IEEE SICE Annual Conference* (2013), pp. 1367–1374.
80. J.L. Rosselló, V. Canals, A. Oliver and A. Morro, Studying the Role of Synchronized and Chaotic Spiking Neural Ensembles in Neural Information Processing, *Int. J. Neural Syst.* **24**(5) (2014) .
81. B. Kriener, H. Enger, T. Tetzlaff, H.E. Plesser, M.-O. Gewaltig and G.T. Einevoll, Dynamics of self-sustained asynchronous-irregular activity in random networks of spiking neurons with strong synapses, *Front. Comput. Neurosci.* **8**(136) (2014) 1–18.
82. A. Knoblauch, F. Hauser, M.-O. Gewaltig, E. Körner and G. Palm, Does spike-timing-dependent synaptic plasticity couple or decouple neurons firing in synchrony?, *Front. Comput. Neurosci.* **6**(55) (2012) 1–27.
83. N.R. Luque, J. a Garrido, R.R. Carrillo, E. D'Angelo and E. Ros, Fast convergence of learning requires plasticity between inferior olive and deep cerebellar nuclei in a manipulation task: a closed-loop robotic simulation, *Front. Comput. Neurosci.* **8**(97) (2014) 1–16.
84. S.L. Reeber, T.S. Otis and R. V Sillitoe, New roles for the cerebellum in health and disease, *Front. Syst. Neurosci.* **7**(83) (2013) 1–11.
85. M. Kronenbuerger, M. Gerwig, B. Brol, F. Block and D. Timmann, Eyeblink conditioning is impaired in subjects with essential tremor, *Brain* **130** (2007) 1538–1551.
86. O. V. Maslennikov and V.I. Nekorkin, Discrete model of the olivo-cerebellar system: Structure and dynamics, *Radiophys. Quantum Electron.* **55**(3) (2012) 198–214.
87. Y. Katori, E.J. Lang, M. Kawato, M. Onizuka and K. Aihara, Quantitative modeling of spatio-temporal

dynamics of Inferior Olive neurons with a simple conductance-based model, *Int. J. Bifurc. Chaos* **20**(3) (2011) 583–603.

88. S. Kitazawa and D.M. Wolpert, Rhythmicity, randomness and synchrony in climbing fiber signals, *Trends Neurosci.* **28**(11) (2005) 611–619.
89. P. Flecknell, Replacement, reduction and refinement, *ALTEX Altern. zu Tierexperimenten* **19**(2) (2002) 73–78.
90. S.H. Frey, L. Fogassi, S. Grafton, N. Picard, J.C. Rothwell, N. Schweighofer, M. Corbetta and S.M. Fitzpatrick, Neurological principles and rehabilitation of action disorders: computation, anatomy & physiology (CAP) model, *Neurorehabil. Neural Repair* **25**(5) (2011) 6S–20S.
91. M. Kawato, S. Kuroda and N. Schweighofer, Cerebellar supervised learning revisited: biophysical modeling and degrees-of-freedom control, *Curr. Opin. Neurobiol.* **21**(5) (2011) 791–800.
92. Y. Hidaka, C.E. Han, S.L. Wolf, C.J. Winstein and N. Schweighofer, Use it and improve it or lose it: Interactions between arm function and use in humans post-stroke, *PLoS Comput. Biol.* **8**(2) (2012) 1–13.
93. N. Schweighofer, Y. Choi, C. Winstein and J. Gordon, Task-Oriented Rehabilitation Robotics, *Am. J. Phys. Med. Rehabil.* **91**(11) (2012) S270–S279.
94. N. Schweighofer, E.J. Lang and M. Kawato, Role of the olivo-cerebellar complex in motor learning and control, *Front. Neural Circuits* **7**(94) (2013) 1–9.
95. I. Laffont, K. Bakhti, F. Coroian, L. van Dokkum, D. Mottet, N. Schweighofer and J. Froger, Innovative technologies applied to sensorimotor rehabilitation after stroke, *Ann. Phys. Rehabil. Med.* **57**(8) (2014) 543–51.